

Microwave Remote Sensing of Palm Swamp Distribution and Flooding Status over a Sub-Region in the Upper Amazon Basin

Podest Erika¹, Pinto Naiara², Schroeder Ronny¹, McDonald Kyle¹, Zimmermann Reiner³, Horna Viviana⁴

¹Jet Propulsion Laboratory, California Institute of Technology, Pasadena, California, USA.

²The University of Maryland, College Park, Maryland, USA.

³University of California Santa Barbara, Santa Barbara, California, USA.

⁴Flathead Lake Biological Station, University of Montana, Polson, Montana, USA.

Abstract- Palm swamp forests are widespread in the Amazon basin. Their combination of permanently saturated soils, warm temperature year-round, and low oxygen soils can lead to a large carbon release. Given their widespread occurrence and expected sensitivity to climate change, it is crucial to develop methods to quantify their spatial extent and inundation state in order to assess their carbon dynamics. These ecosystems are remote and inaccessible but spaceborne microwave remote sensing can effectively characterize them because of its sensitivity to surface water and vegetation structure and inaccessible areas can be monitored regularly regardless of weather or day/night conditions.

We developed a remote sensing methodology using microwave data to determine palm swamp distribution and inundation state over a sub-region in northern Peru. High-resolution (100m) SAR data and coarse resolution 25km active/passive microwave data were used synergistically to characterize palm swamp extent, and flooding status.

Key Words: wetlands, palm swamps, inundation, microwave remote sensing

1. INTRODUCTION

Palm swamp forests cover large regions of the Amazon Basin, estimated to be over 50,000 km² (Eva *et al.*, 2002). These wetland ecosystems form where seasonal flooding is moderate but surface inundation remains constant. The combination of permanently saturated soils, warm temperature year-round, and low oxygen in palm swamp soils can lead to large amounts of carbon release to the atmosphere, particularly as methane, whose warming potential as a greenhouse gas is 23 times higher than that of CO₂ (IPCC, 2001). Little is known however on the contribution of palm swamps to the overall carbon balance of the basin. In this context, the incomplete knowledge about the biogeochemistry of palm swamps has been addressed as one of the largest sources of uncertainty for understanding the global CH₄ cycle (Wania *et al.*, 2004). Current models have been unable to predict the high concentrations of measured atmospheric methane over some areas of tropical rainforests in the equatorial regions of South America and Africa (Bergamaschi *et al.*, 2007; Frankenberg *et al.*, 2005). Disagreements between measured and modeled data are particularly large in the Upper Amazon, which is, for modeling purposes, classified as a “*terra firme* pre-humid rainforest” (Prigent *et al.*, 2001a; Walter *et al.*, 2001). *Terra firme* forests are known to release no methane to the atmosphere. This mis-classification of vegetation functional type within the models, the uncertainties in the extent and distribution of the palm

swamps, and the associated error in the model-based carbon flux estimates, completely neglect CH₄ release of the palm swamps in this region and may be one of the important missing pieces of the tropical CH₄ budget. If the palm swamps found in the upper Amazon constitute a significant methane source, and if this methane release persists most of the year, fostered by high ecosystem productivity, then appropriate information on the regional distribution and seasonal inundation state of these ecosystems will contribute key information for use in ecosystem process modeling to resolve the discrepancy between global methane models and atmospheric concentration measurements. Because of the widespread occurrence and expected sensitivity to climate change of these ecosystems, it is crucial to develop methods to quantify their spatial extent and inundation state. Precise information on the extent and characteristics of palm swamps is difficult to gather because of their remoteness and difficult accessibility. Remote sensing is a unique tool to study and monitor these ecosystems especially through the use of radar, which provides the capability of acquiring images regardless of day/night conditions or the presence of clouds, which are especially prevalent in tropical regions.

We have developed a remote sensing methodology to characterize palm swamp distribution and inundation state over a focus area in the upper Amazon (Figure 1).

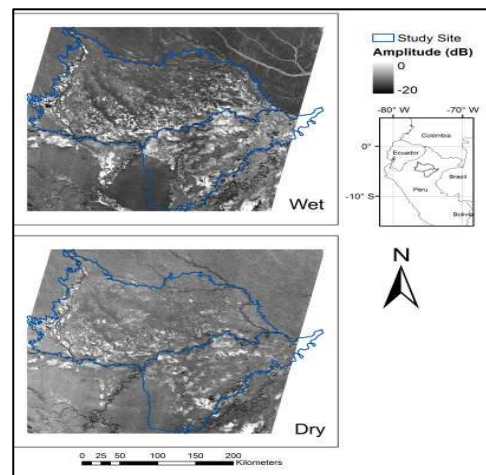


Figure 1. The Loreto study site, in the upper Amazon of Northern Peru, is delineated on the ALOS/PALSAR multi-temporal image mosaics of the area.

Current satellite microwave remote sensing capabilities allow for either mapping of wetlands at high spatial resolutions (~30-100 m scale) with synthetic aperture radar's (SAR's) having temporally sparse observations of 4-6 weeks (e.g Whitcomb *et al.*, 2009; Hess *et al.*, 2003; Hess *et al.*, 1990), or for relatively high temporal fidelity

(daily observation with ~weekly -to -monthly composites) with coarse spatial resolutions (~25–50 km) (e.g Prigent *et al.*, 2001b; Grippa *et al.*, 2007; Mialon *et al.*, 2005) with scatterometers or passive microwave sensors. In this study we used the capabilities of high resolution SARs and of coarse resolution active and passive spaceborne microwave remote sensing instruments to determine (1) palm swamp forest distribution and (2) flooding regime and inundation dynamics. These factors are critical in determining methane exchange rates for these ecosystems.

We have developed and tested our remote sensing classification algorithms over a focus area in the upper Amazon (Figure 1) where ground data is under way and a baseline classification map is available.

2. SITE AND DATA COLLECTION

Our study site is located in the upper Amazon in Northern Peru, near Loreto (Figure 1). The inundated areas in the study site contain a mix of grasslands, trees and palm swamps. *Terra firme* forests are found in dry areas and successional regrowth areas (*cecropia*) are found in dry patches near rivers and having large disturbances. A Landsat based classification map derived by the Peruvian geographers was used as a guide to validate our results.

The combination of SAR, scatterometer, and passive microwave data was acquired as part of our involvement in assembling a global scale Earth System Data Record (ESDR) of inundated wetlands under a NASA MEaSUREs project (PI-McDonald). Under MEaSUREs, data from both high and low spatial resolution microwave sensors is being assembled over critical wetland regions, including the Amazon Basin. The high spatial resolution data is comprised of L-band SAR from ALOS PALSAR (available as of 2006 and launched by the Japanese Space Agency-JAXA), which include yearly full continental-scale coverage for dual polarization (HH and HV) fine beam and multiple acquisitions of HH-pol ScanSAR at 17-46-day repeat cycles for at least one year, both products at 50 meter spatial resolution. Also under MEaSURE's and other NASA related activities, we have acquired global coarse resolution (~25 km) datasets from QuikSCAT scatterometer and AMSR-E passive microwave data covering time periods contemporaneous with PALSAR over the Amazon Basin.

3. METHODOLOGY

Through an unsupervised approach we developed a wetland distribution map at high spatial resolution (approx. 90 meters) using a combination of L-band SAR data from ALOS PALSAR, complemented with a digital elevation model (DEM) from the Shuttle Radar Topography Mission (SRTM). The unsupervised classifier consisted of K-means classifier.

Landscape inundation fraction at the 25 km scale was generated through a mixing model (based on end members) from passive and active microwave satellite data from AMSR-E (18.7 GHz channel) and QuikSCAT

(13.4 GHz channel) that provide daily coverage of the study region (Schroeder *et al.*, 2010).

4. RESULTS AND DISCUSSION

ALOS PALSAR multi-temporal Scansar images were acquired (HH polarization only) for our site of interest in the Loreto area (Table 1). The images were received terrain corrected and geocoded to a 90-meter resolution, matching the SRTM digital elevation model (DEM). The Scansar images have a temporal distribution that capture the flood pulse, with a maximum flood extent in March-April and a minimum extent in September.

Table 1: ALOS/PALSAR images covering the Loreto study area

File Name	Acquisition Date
20070129_445_HH_004_18M.tc.fine.geo.mli	Jan 1 st , 2007
20070316_445_HH_005_18M.tc.fine.geo.mli	Mar 3 rd , 2007
20070501_445_HH_005_18M.tc.fine.geo.mli	May 1 st , 2007
20070616_445_HH_002_18M.tc.fine.geo.mli	Jun 16 th , 2007
20070801_445_HH_002_18M.tc.fine.geo.mli	Aug 1 st , 2007
20070916_445_HH_002_18M.tc.fine.geo.mli	Sep 16 th , 2007
20090321_445_HH_001_18M.tc.fine.geo.mli	Mar 21 st , 2009
20090621_445_HH_001_18M.tc.fine.geo.mli	Jun 21 st , 2009
20091222_445_HH_001_18M.tc.fine.geo.mli	Dec 22 nd , 2009

The classifier was an unsupervised K-means approach in order to identify homogeneous areas and correlate classes with the baseline Landsat derived classification map on hand. A series of ancillary datasets were input into the classifier: 1) a SRTM DEM, (3-arcsecond- Figure 2), 2) temporal mean of all PALSAR images (average signal- Figure 2) 3) temporal variation of all PALSAR images (standard deviation), 4) Lee filtered images (each image was applied the Lee filter), and 5) textures (variance, skewness, and entropy) for each image using 5x5, 7x7, and 11x11 window sizes.

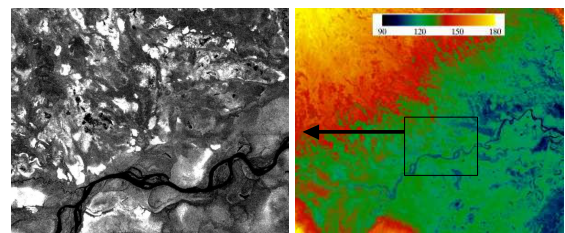


Figure 2: Left-HH Scansar, average of 9 dates covering 2007 and 2009. Right- 90m SRTM DEM of the area.

The following two classifications were initially performed: 1) the entire multi-temporal PALSAR stack to obtain temporal inundation dynamics and 2) each PALSAR image to characterize each acquisition date, see Figure 3. Eight classes and ten iterations were found optimal to identify palm swamp forest patches and discern flooded vegetation from *terra firme* forests.

The main challenge in the classification effort was to separate inundated vegetation from palm swamp forests. The time frame of the Landsat image used to generate the

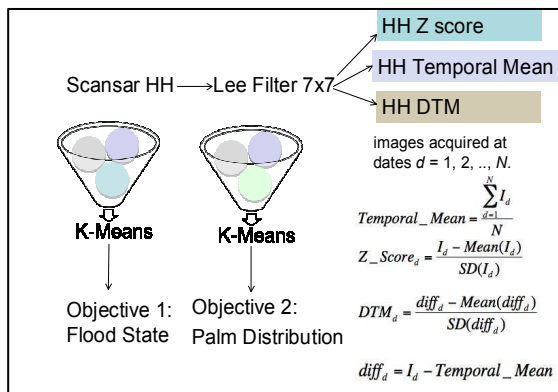


Figure 3: Unsupervised K-means classification approach.

wetland classification map was unknown. Some land cover patterns varied significantly between the Landsat classification and the radar classification. In addition, visual inspection of the Landsat classification suggested that there was significant variation in the “mixed palm swamp forest” class, possibly due to grasses and different degree of sediment exposure. The variation in inundation pattern further complicated this pattern.

Signatures for flooded vegetation (FV), open water (OW), and dry (DRY) areas were obtained for our study site. The signatures were obtained after masking out areas having a slope greater than 3 degrees and an elevation greater than 300 meters. Figure 4 shows and example of the signature extraction for a single date.

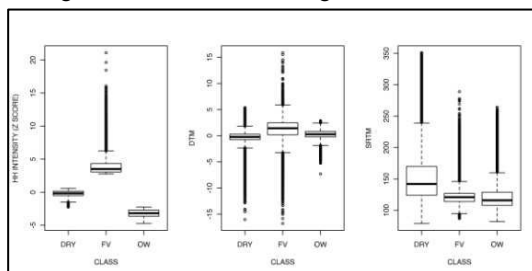


Figure 4: Signatures for flooded vegetation (FV), open water (OW), and dry (DRY) areas in Loreto, Peru for date March 16, 2007.

The signatures for flooded vegetation, open water, and dry areas were consistent among seasons and acquisition dates. *Terra firme* was differentiated from flooded forests and the K-means classification approach was useful for inferring signatures in the absence of ground reference data. Dense palm swamps patches were more accurately identified than sparse patches. The latter were more often classified as flooded forest or flooded grass. Figure 5 shows the resulting classification distinguishing palm swamp forests from open water and dry land.

Landscape inundation fraction, derived at 25 km resolution from AMSR-E and QuikScat over the area of interest (Figure 6) were harmonized with the high resolution SAR derived products. Results show high correlation in areas of open water and to a lesser degree over areas of high biomass flooded forests.

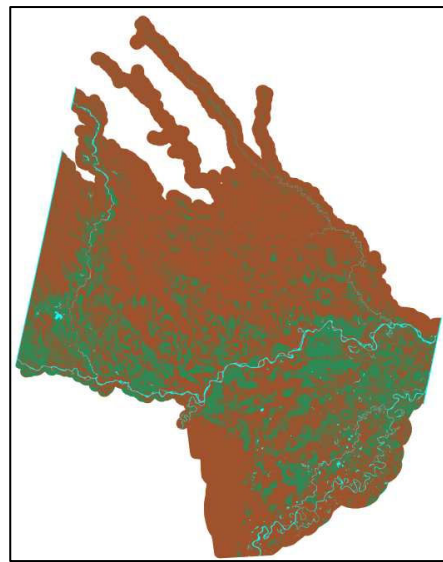


Figure 5: Classification results of the Loreto floodplain. Green = palm swamps, blue = open water, brown = other classes. 20300 km² are predicted to be covered by palm swamps

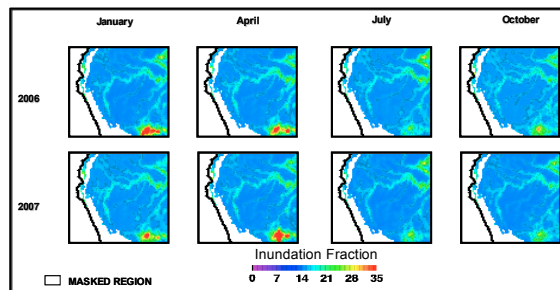


Figure 6: Combined QuikSCAT and AMSR-E microwave data to generate landscape inundation fraction (shown at percent inundated areas of 25km grid cells) comparing the upper Amazon Basin in northern Peru for 4 different months over 2006 and 2007.

5. CONCLUSION

Classification results show that improvements still need to be performed in terms of excluding shadows and avoiding misclassification in areas of steep terrain and in obtaining better separability between dense and sparse palm swamp forest patches. The next step is running a supervised decision tree classification approach based on the classes identified through the unsupervised approach.

REFERENCES

- Bergamaschi, P., Frankenberg, C., Meirink, J.F., Krol, M., Dentener, F., Wagner, T., Platt, U., Kaplan, J. O., Koerner, S., Heimann, M., Dlugokencky, E. J. & Goede, A., **2007**, Satellite cartography of atmospheric methane from SCIAMACHY on board ENVISAT: 2. Evaluation based on inverse model simulations. *Journal of Geophysical Research-Atmospheres* 12, D02304.
- Eva, H.D., de Miranda, E.E., Di Bella, C.M., Gond, V., *et al.*, **2002**, A Vegetation map of South America, European Commission, Luxembourg.
- Frankenberg, C., Meirink, J.F., van Weele, M., Platt, U. & Wagner, T., **2005**, Assessing methane emissions from global space-borne observations. *Science* 308, 1010-1014.

Grippa, M., Mognard, N., Le Toan, T., and Biancamaria, S., **2007**, Observations of changes in surface water over the western Siberia lowland, *Geo Res. Letters*, 34, L15403, doi:10.1029/2007GL030165.

Hess, L., J.M. Melack, E.M. Novo, C.C.F. Barbosa, and M. Gastil, **2003**. "Dual-Season Mapping of Wetland Inundation and Vegetation for the Central Amazon Basin," *Remote Sensing of Environment*, 87, pp. 404-428.

Hess, L. L., Melack, J. M., and Simonett, D. S., **1990**, Radar detection of flooding beneath the forest canopy: a review. *International Journal of Remote Sensing*, 11, pp. 1313-1325.

IPCC (2007): Fourth Assessment Report. Climate Change, **2007**, http://www.ipcc.ch/pdf/assessment-report/ar4/syr/ar4_syr_topic1.pdf

Mialon, A., Royer, A., and Fily, M., **2005**, Wetland seasonal dynamics and internannual variability over northern high latitudes, derived from microwave satellite data, *Journal of Geophysical Research*, 110, D17102, doi:17110.17129/12004JD005697.

Prigent, C., E. Matthews, F. Aires, and W.B. Rossow, **2001a**, Remote sensing of global wetland dynamics with multiple satellite data sets. *Geophys. Res. Lett.*, 28, 4631, doi:10.1029/2001GL013263.

Prigent, C., Aires, F., Rossow, W. B., and Matthews, E., **2001b**, Joint characterization of vegetation by satellite observation from visible to microwave wavelength: A sensitivity analysis, *Journal of Geophysical Research*, 106, pp. 20665-20685.

Schroeder, R. M. A. Rawlins, K. C. McDonald, E. Podest, R. Zimmermann and M. Kueppers, **2010**. Satellite Microwave Remote Sensing of North Eurasian Inundation Dynamics: Development of Coarse-Resolution Products and Comparison with High-Resolution Synthetic Aperture Radar Data. *Environmental Research Letters, special issue on Northern Hemisphere high latitude climate and environmental change*, **5** (2010) 015003 (7pp) doi:10.1088/1748-9326/5/1/015003.

Walter, K.M., Zimov, S.A., Chanton, J.P., Verbyla, D. & Chapin, F.S., **2006**, Methane bubbling from Siberian thaw lakes as a positive feedback to climate warming. *Nature* 443, 71-75.

Wania, R., Prentice, C., Harrison, S., Hornibrook, E., Gedney, N., Christensen, T. & Clymo, R., **2004**, The role of natural wetlands in the global methane cycle. *EOS* 85, 466.

Whitcomb, J.M., M. Moghaddam, K. McDonald, J. Kellndorfer, and E. Podest, **2009**. "Mapping vegetated wetlands of Alaska using L-band radar satellite imagery," *Canadian Journal of Remote Sensing*, Vol 35 No. 1, pp. 54-72.

ACKNOWLEDGEMENTS

Portions of this work were carried out at the Jet Propulsion Laboratory, California Institute of Technology, under contract with the National Aeronautics and Space Administration. This work has been undertaken in part within the framework of the JAXA ALOS Kyoto & Carbon Initiative. ALOS PALSAR data have been provided by JAXA EORC. The Level 2A QuikSCAT and Level 2A AMSR-E data were provided by the NASA Jet Propulsion Laboratory Physical Oceanography DAAC.

© 2011. All rights reserved